JACS
JOURNAL OF THE AMERICAN CHEMICAL SOCIETY

Article

pubs.acs.org/JACS

Mechanisms for CO Production from CO_2 Using Reduced Rhenium Tricarbonyl Catalysts

Jay Agarwal,[†,‡] Etsuko Fujita,[‡] Henry F. Schaefer, III,*[,†] and James T. Muckerman*[,‡]

[†]Center for Computational Quantum Chemistry, University of Georgia, Athens, Georgia 30602, United States

[‡]Chemistry Department, Brookhaven National Laboratory, Upton, New York 11973, United States

Supporting Information

ABSTRACT: The chemical conversion of CO_2 has been studied by numerous experimental groups. Particularly the use of rhenium tricarbonyl-based molecular catalysts has attracted interest owing to their ability to absorb light, store redox equivalents, and convert CO_2 into higher-energy products. The mechanism by which these catalysts mediate reduction, particularly to CO and $HCOO^-$, is poorly understood, and studies aimed at elucidating the reaction pathway have likely been hindered by the large number of species present in solution. Herein the mechanism for carbon monoxide production using rhenium tricarbonyl catalysts has been investigated using density functional theory. The investigation presented proceeds from the experimental work of Meyer's group (*J. Chem. Soc., Chem. Commun.* **1985**, 1414−1416) in DMSO and Fujita's group (*J. Am. Chem. Soc.* **2003**, 125, 11976−11987) in dry DMF. The latter work with a simplified reaction mixture, one that removes the photo-induced reduction step with a sacrificial donor, is used for validation of the proposed mechanism, which involves formation of a rhenium carboxylate dimer, $[Re(dmb)(CO)_3]_2(OCO)$, where dmb = 4,4′-dimethyl-2,2′-bipyridine. CO_2 insertion into this species, and subsequent rearrangement, is proposed to yield CO and the carbonate-bridged $[Re(dmb)(CO)_3]_2(OCO_2)$. Structures and energies for the proposed reaction path are presented and compared to previously published experimental observations.

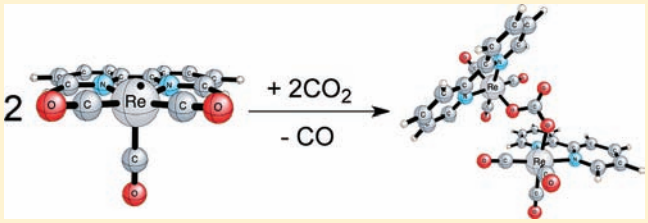

INTRODUCTION

The utilization of carbon dioxide is a primary environmental objective due to its role as a greenhouse gas.[1−8] The abundance of CO_2 also makes it an attractive feedstock, similar to H_2O and N_2, but the thermodynamic stability of these species makes chemical conversion an energy-intensive process.[9] With regard to CO_2, several metal-centered catalysts are capable of mediating chemical conversion to higher-energy products, including nickel,[10−16] cobalt,[11,17−24] ruthenium,[25−32] rhenium,[33−38] and iron[18,39−41] complexes. The work herein is focused on rhenium tricarbonyl photocatalysts, in particular $[fac\text{-}Re(2,2'\text{-bipyridine})(CO)_3X]^n$, where the bipyridine may be bare or functionalized and X is an axial ligand such as a halide ($n = 0$) or a solvent molecule ($n = +1$). Herein we use "axial" to describe ligands perpendicular to the "equatorial" plane formed by bipyridine, the metal, and two carbonyl ligands. Prior work has shown that this catalyst, once irradiated in a CO_2-saturated solvent, yields two products: CO (major) and $OCHO^-$.[33,36,42−45] The mechanisms for product formation, however, are not well understood.

Mechanistic studies are hindered in part by the large number of species present in solution, especially in the case of photochemical reduction with a sacrificial electron donor, which makes spectroscopic analysis difficult. Since catalytic CO_2 reduction is preceded by reduction of the metal center, sacrificial donors must be included in solution to quench the excited metal center after irradiation. These sacrificial species, often tertiary amines, are added in excess, and the oxidized, open-shell products participate in several decomposition pathways.[46,47] Subsequent byproducts continue to react with species in solution, which makes elucidation of the specific reaction path difficult. Previously, amines have been proposed as both proton and electron sources for reduction,[48−50] but CO_2 can also be reduced in the absence of such species.[33,51]

We note that in published mechanistic studies, several steps have been observed after the metal center has been reduced.[19,33,51] First the axial ligand (X) dissociates, leaving a 5-coordinate (17 e^-) complex. This neutral radical is trapped by coordinating solvents such as acetonitrile and dimethylformamide (DMF) to form a 6-coordinate ("19 e^-") species with the unpaired electron on the bipyridine ligand. An equilibrium between the 5- and 6-coordinate species allows for potential CO_2 coordination at the axial position.[52] Further steps have been postulated in previous experimental publications to include dimer formation,[33] carboxylic acid formation,[53] and/or outer-sphere electron transfer.[43]

One way to simplify the reaction is to remove the photoexcitation step. This can be achieved by monitoring CO_2 reduction on an electrode-immobilized catalyst, or a catalyst in a solution with supporting electrolyte using an electrochemical method.[54,55] Alternatively, the one-electron-

Received: November 10, 2011
Published: February 23, 2012

dx.doi.org/10.1021/ja2105834 | *J. Am. Chem. Soc.* 2012, 134, 5180−5186

Scheme 1. Proposed Reduction Pathway

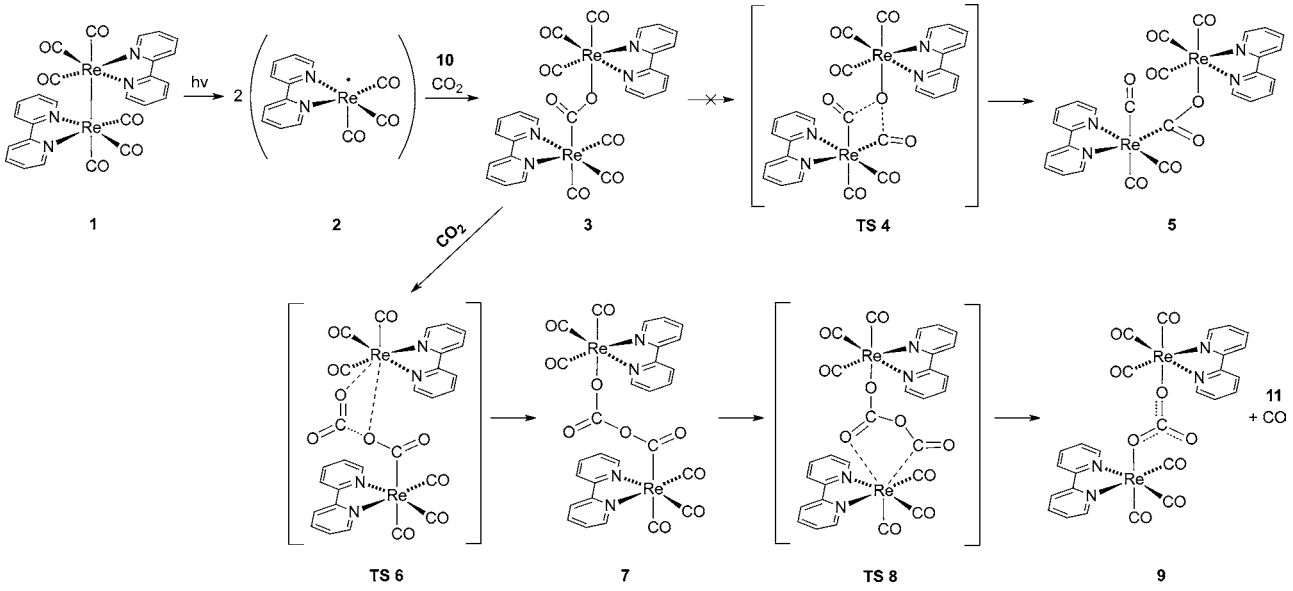

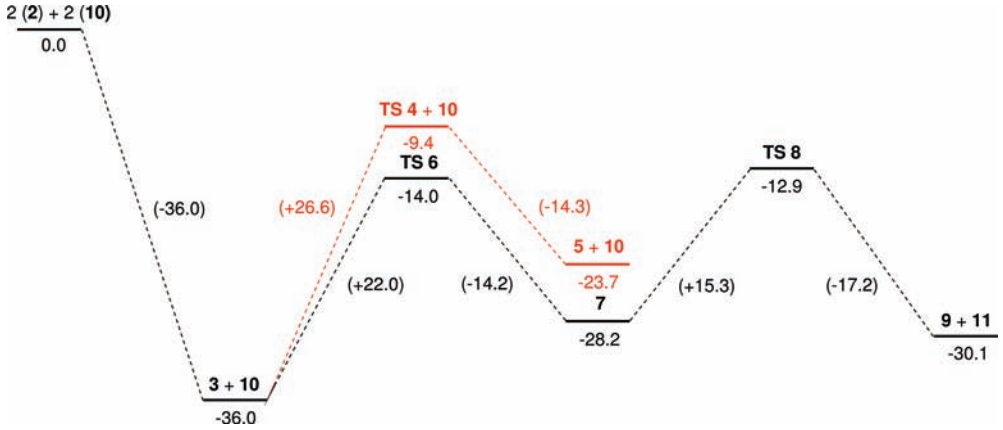

Figure 1. Standard enthalpy profile. ΔH^*(DMF) energies shown in kcal mol^{-1}. The isomerization of **3** is indicated in red.

reduced (OER) center can be prepared by photocleavage of a Re−Re dimer in a CO_2-saturated solvent.[33] We have focused on studies using the latter, which mitigates the inclusion of excess electrolyte but forgoes the catalytic cycle. Thus, the reactants are simply the OER rhenium catalyst [where the active species is Re(bpy)$(CO)_3^{\bullet}$], CO_2, and solvent.

Of special interest to us is the experimental work of Hayashi, Kita, Brunschwig, and Fujita, who prepared the OER rhenium catalyst by photocleaving the Re−Re bond of [Re(dmb)-$(CO)_3]_2$, where dmb = 4,4′-dimethyl-bpy, which was prepared using Na−Hg reduction.[33] Briefly, they observed that several products formed in CO-saturated DMF: carbon monoxide, a rhenium carbonate dimer, [Re(dmb)$(CO)_3]_2(OCO_2)$, and Re(dmb)$(CO)_3(OCO_2H)$. They were also able to observe a long-lived intermediate, [Re(dmb)$(CO)_3]_2(C(O)O)$, using NMR. This species decomposes with a rate that is first-order in [CO_2] and produces CO with a 25−50% yield based on [Re]. From this work we propose a mechanistic pathway for CO production that begins with the formation of a rhenium carboxylate dimer, as observed, and proceeds with CO_2 insertion into the rhenium−oxygen bond. We present energies and structures from our density functional theory (DFT) investigation in the following sections.

THEORETICAL METHODS

All computations were performed using DFT as implemented in Gaussian 09.[56] Geometry optimization and vibrational analysis were computed in the gas phase. Molecular size precluded geometry optimization with implicit solvent, but solvation was included in subsequent single-point energy computations using the polarizable continuum model (CPCM) with default parameters for DMF.[57,58] Stationary points were verified using vibrational analysis, and transition-state structures were connected to minima using intrinsic reaction coordinate computations.[59−61]

We chose to employ the popular B3LYP functional, which includes Becke's three-parameter hybrid functional with the Lee−Yang−Parr correction for correlation.[62−64] Additionally, we have included energy values computed with M06-L, a local density functional recently developed by Zhao and Truhlar.[65] Prior work has shown that these functionals are appropriate for studying complexes containing transition metals,[66−69] and for rhenium specifically.[70,71]

To parametrize the rhenium center we chose the LANL08F basis set with Hay−Wadt relativistic effective core potential. In prior work, this uncontracted triple-ζ-quality basis set has been shown to provide an appropriate description of rhenium's core and valence shells.[71−73] For light atoms (H, C, N, and O), the 6-31++G(d,p) Pople basis set was used.[74,75] Where appropriate, a correction was applied to account for the standard state of 1 M for non-gases in solution.

dx.doi.org/10.1021/ja2105834 | J. Am. Chem. Soc. 2012, 134, 5180−5186

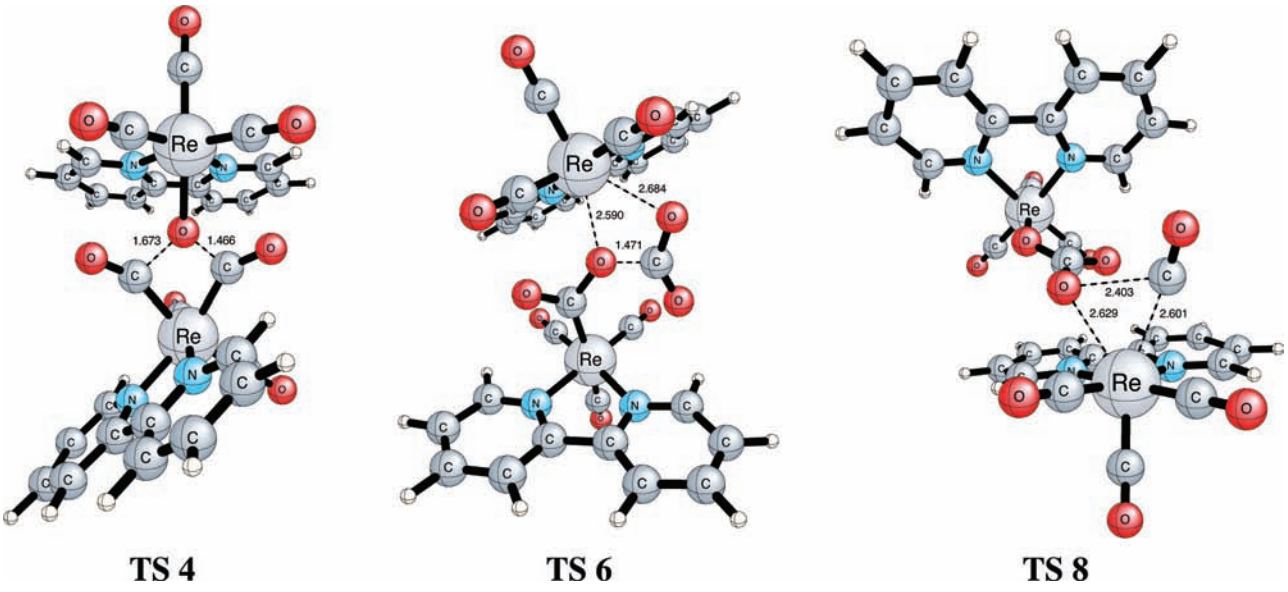

Figure 2. Optimized geometries for the isomerization, CO_2 insertion, and rearrangement transition-state structures. Bond lengths shown in Angstroms. Geometries were optimized at the B3LYP/LANL08F (Re), 6-31++G(d,p) (H, N, C, O, Cl) level of theory.

RESULTS AND DISCUSSION

Our proposed mechanism for CO production is outlined in Scheme 1. We first discuss the pathways that are depicted in this scheme before relating them to experiment. Relative standard enthalpies for the reaction steps shown in Scheme 1 are listed in Table 1, with a depiction of the energy profile shown in Figure 1. Geometries for the transition state structures are shown in Figure 2. We reference the solvent-phase M06-L enthalpies in our discussion, but provide additional results from computations using B3LYP and M06-L functionals for later comparison.

Mechanism. Our investigation begins with the OER rhenium catalyst, **2**, which is formed regardless of the reduction mechanism. That is, $Re(bpy)(CO)_3^{\bullet}$ may be formed from photocleavage of the Re−Re bond in **1**, the one-electron reduction of $Re(bpy)(CO)_3X$ using an electrical bias, or the photochemical reduction of $Re(bpy)(CO)_3X$ using tertiary amines. This OER species exists in an equilibrium between the 5- and 6-coordinate configurations, the latter having been solvated by a coordinating solvent. In the 5-coordinate arrangement there is a vacant coordination site at an axial position that allows for CO_2 coordination. In the event that two OER centers are in the proximity of CO_2 (**10**), a carboxylate dimer, **3**, may form. This process is not favored entropically, however, as three bodies must converge to one, but we find that it is a significantly exothermic step (-36.0 kcal mol^{-1}).

The geometry of **3** is a skewed "trans" configuration with respect to the bipyridine rings; the bipyridine ligands oppose each other but are not parallel, so no symmetry plane exists. In our investigation we considered the rotation of the monomer units around the bridging CO_2 moiety while searching for the lowest-energy structure by considering "cis", "trans", and skewed arrangements, but in each case optimization yields a skewed "trans" minimum. From further analysis we found that the dimer may then follow two potential pathways: one leading to isomerization and the other to CO_2 insertion. We are primarily concerned with the latter, but briefly discuss the former.

Isomerization of **3** proceeds through **TS4**. The original dimer, **3**, contains a bridged CO_2 species, with a carbon atom bound at the axial position of one rhenium center and an oxygen atom bound at the axial position of the other. The first step of isomerization is formation of a bond between the rhenium-bound oxygen of CO_2 and an equatorial carbonyl ligand coordinated to the opposing rhenium center. This yields the transition state **TS4**. Next, the original oxygen−carbon bond in the bridging CO_2 species is cleaved, leaving a carbonyl ligand at the axial position of one rhenium center. After cleavage, the rhenium centers are still bridged by CO_2, but with an oxygen atom bound at the axial position of one rhenium center and a carbon atom bound at the equatorial position of the other. There exists a high activation barrier to this process (26.6 kcal mol^{-1}), and the isomerization is overall endothermic by 12.3 kcal mol^{-1}. Thus the original dimer, **3**, is favored.

If an additional CO_2 molecule is available in solution, it may insert into the carboxylate dimer, **3**, at the rhenium−oxygen bond. CO_2 insertion is a stepwise process beginning with the insertion transition-state **TS6**, leading to **7**, a local minimum. The complex then rearranges through **TS8** to yield **9**. It is important to note that the initial insertion step mirrors that of CO_2 insertion into a rhenium−hydride bond.[50,76] In both cases the carbon atom of the attacking CO_2 molecule acts as a Lewis acid, and forms a covalent bond with the electron-rich axial ligand bound to rhenium. At the same time, an oxygen atom of CO_2 donates a lone pair of electrons to form a rhenium−oxygen dative bond. In the case of the dimer, the electron-rich ligand is an oxygen atom that belongs to the bridging CO_2 species. This first step yields **7**, a dimer with an elongated bridging ligand consisting of two CO_2 monomers. Insertion, therefore, may be viewed as the oligomerization of CO_2. Importantly, the activation barrier to forming **TS6** (22.0 kcal mol^{-1}) is lower than that of isomerization. Overall this step is endothermic by 7.8 kcal mol^{-1}.

Following insertion, the new dimer complex, **7**, undergoes rearrangement. This is a critical step that yields carbon monoxide. The rearrangement step involves migration of one rhenium center from the carbon atom of the original CO_2 to

dx.doi.org/10.1021/ja2105834 | J. Am. Chem. Soc. 2012, 134, 5180−5186

the oxygen atom of the attacking CO_2. The result of this process is cleavage of a carbon−oxygen bond within the original CO_2 to yield CO (**11**), in addition to CO_3, which has a formal −2 charge (i.e., carbonate) and bridges the two Re(I) centers to yield **9**. The activation barrier for this step, through **TS8**, is 15.3 kcal mol^{-1}. This process, **3** + **10** → **9** + **11**, is endothermic by 5.9 kcal mol^{-1}. Overall the two steps of the insertion process can be viewed as disproportionation of two CO_2 molecules with two electrons (one from each of the two Re centers) to yield carbonate and carbon monoxide.

Tryk and co-workers previously investigated electrochemical CO_2 reduction using metal-supported nanoporous activated carbon fiber electrodes in aqueous $KHCO_3$.[77] They proposed the involvement of $(CO_2)_2^{\bullet-}$ formed by the reaction of CO_2 with $CO_2^{\bullet-}$. Subsequent reduction of this species forms $(CO_2)_2^{2-}$, which produces CO and CO_3^{2-} by disproportionation. Our system also produces $(CO_2)_2^{2-}$ [in the form of Re^I-$(CO_2)_2^{2-}$-Re^I], but from the direct two-electron reduction of CO_2 rather than through a radical intermediate.

Another way to describe the insertion process is through the movement of electrons. The initial metal−metal dimer, **1**, is a neutral complex with a 34-electron dinuclear core. Homolytic cleavage of the weak Re−Re bond in this dimer yields two 5-coordinate, 17-electron monomers that are neutral radicals. As mentioned, the monomer exists in an equilibrium between the 5-coordinate 17-electron species and the solvated, 6-coordinate "19-electron" species with the unpaired electron on the bipyridine ligand.

The carboxylate dimer, **3**, forms through the addition of the two radical Re metal centers across a CO double bond to give CO_2^{2-} with a bent structure. Thus each metal center is oxidized by one electron, leaving each rhenium with a +1 formal charge. Overall, the carboxylate dimer is a neutral singlet.

Insertion of an additional CO_2 into **3** of course has no effect on the overall charge. The two electrons that form a dative bond between the oxygen atom of CO_2 and the rhenium center are used to form a covalent bond with the carbon atom of the inserting CO_2 molecule. Subsequently a double bond in the attacking CO_2 breaks heterolytically, which allows for a dative bond to form between a new oxygen atom and rhenium. Therefore, the two electrons that originated from the reduced metal centers are still contained within the bridging moiety, which has a formal −2 charge. Disproportionation of this moiety through rearrangement yields neutral CO and the dianion CO_3^{2-}, which bridges the two cationic metal centers to yield the neutral dimer **9**. It is important to note that the first equivalent of CO_2, the one used to form **3**, contains the carbon atom that is part of the CO product. The second equivalent of CO_2, on the other hand, contains the carbon atom that becomes part of the CO_3^{2-} moiety in **9**.

Comparison to Experimental Work. Sullivan and co-workers[51] and Hayashi and co-workers[33] have both studied the reduction of CO_2 using a reduced Re−Re dimer. Homolytic cleavage of the weak metal−metal bond in this species yields two neutral radical monomers, which react with CO_2. The same monomer is produced in photocatalytic reduction, but requires the presence of sacrificial donors in solution. As mentioned, removing the photoreduction step has the consequence of eliminating the catalytic cycle, but the benefit of greatly simplifying the reaction mixture.

To produce the reduced rhenium dimer, Sullivan and co-workers began with $Re_2(CO)_{10}$. In a reflux of xylenes and 2,2′-bipyridine (bpy), they exchanged four CO ligands for the bidentate bpy to produce **1**. Conversely, Hayashi and co-workers started with two rhenium monomers, Re(dmb)-$(CO)_3$OTf, and reduced them with Na−Hg amalgam to produce $[Re(dmb)(CO)_3]_2$. In either case, the neutral radical monomer can be produced from the metal−metal dimer, and a CO product is observed when using a CO_2-saturated solvent. It is important to note that for our investigation we have used bpy, like Sullivan and co-workers, instead of dmb, like Hayashi and co-workers, in an effort to reduce the size of our computations. Therefore, in the following discussion we refer to our structures in Figure 1 for simplicity, in spite of the fact that they contain bare rather than functionalized bpy ligands.

Sullivan and co-workers carried out experiments with the reduced dimer in CO_2-saturated dimethylsulfoxide. They observed CO and Re(bpy)$(CO)_3$(OC(O)OH) as products, but were unable to observe intermediates. They conjectured that it was possible that the radical monomers, **2**, reacted directly with CO_2. Hayashi and co-workers began with a similar experiment, employing the Re−Re dimer in a $^{13}CO_2$-saturated solution of DMF with incident irradiation. By monitoring the reaction with ^{1}H NMR, ^{13}C NMR, FTIR, and GC, they were able to identify ^{13}CO, $[Re(dmb)(CO)_3]_2(O^{13}CO_2)$, and Re(dmb)$(CO)_3(O^{13}C(O)OH)$ as products. They note that the Re(dmb)$(CO)_3$(OC(O)OH) product, left to stand, converts to $[Re(dmb)(CO)_3]_2(OCO_2)$. Importantly, they did not observe H_2, ^{12}CO, or $HCOO^-$ production, but identified the carboxylate dimer $[Re(dmb)(CO)_3]_2(O^{13}CO)$ as a long-lived intermediate.

Our proposed insertion pathway agrees well with the experimental observations. To begin, we find that the first equivalent of CO_2 bridges two reduced monomers, **2**, to form **3**. While a carboxylate bridge could conceivably be formed through other routes, the observation of $[Re(dmb)(CO)_3]_2(O^{13}CO)$ using $^{13}CO_2$ indicates that the first equivalent of CO_2 becomes the bridging species. From **3**, we predict the activation barrier for isomerization or insertion to be relatively high (>20 kcal mol^{-1}), adding to the stability of the carboxylate dimer as a long-lived intermediate. The high barrier to insertion (21.5 kcal mol^{-1}), which is the energetically favored route, also agrees with the relatively slow reaction rate of 0.003 s^{-1}.[33] Similarly, the decay of $[Re(dmb)(CO)_3]_2(O^{13}CO)$ is first-order in $[^{13}CO_2]$;[33] therefore formation of the products ^{13}CO and $[Re(dmb)(CO)_3]_2(O^{13}CO_2)$ agrees with our proposed insertion step, **3** + **10** → **TS6**, which is required for CO production.

Subsequent rearrangement of the dimer with an -O(CO)O-(CO)- bridge, **7**, may be difficult to observe experimentally. The activation barrier for this step, **7** → **TS8**, is modest (16.5 kcal mol^{-1}), and rearrangement is overall slightly exothermic (−0.3 kcal mol^{-1}). Again, this step is supported by experimental observations. We find that both of the products, **9** and **11**, contain carbon atoms from added CO_2 equivalents. Therefore, if $^{13}CO_2$ is employed, the carbonate moiety of **9** and the CO product, **11**, should be ^{13}C-labeled. This aligns with the observations of Hayashi and co-workers, who observed $[Re(dmb)(CO)_3]_2(O^{13}CO_2)$ and ^{13}CO using $^{13}CO_2$.[33]

More importantly, Hayashi and co-workers[33] did not observe ^{12}CO when employing $^{13}CO_2$. This eliminates the possibility that CO production is the result of ligand dissociation. Initially we had considered the possibility of a tetracarbonyl intermediate, Re(bpy)$(CO)_4^+$, but the presence of both isotope-labeled and unlabeled axial carbonyl ligands should produce both labeled and unlabeled CO products. This is an

dx.doi.org/10.1021/ja2105834 | J. Am. Chem. Soc. 2012, 134, 5180−5186

important argument against the isomerization pathway, which we predict to be energetically unfavorable. The isomerization product **5** contains axial CO ligands that could dissociate to yield CO, but would yield both labeled and unlabeled products when employing $^{13}CO_2$. Furthermore, isomerization would form a dimer with an unlabeled carboxylate bridge, which does not match experimental observations. We did, however, "probe" the isomerized dimer for reaction with an additional equivalent of CO_2 at the carbon and oxygen atoms of the carboxylate bridge, but observed dissociation of the added CO_2 (i.e., no reaction) in each case. Conversely, we cannot account for the small amount of Re(dmb)$(CO)_3$(OC(O)OH) that is observed. The formation of this species requires a proton source, likely trace water in solution.

Energetics. Standard enthalpies of reaction computed with the B3LYP and M06-L functionals are presented in Table 1. As

Table 1. Relative Enthalpies for Steps of the Present Mechanism for Given DFT Functionals[a]

	B3LYP		M06-L	
reaction step	$\Delta H°$(gas)	$\Delta H°$(DMF)[b]	$\Delta H*$(gas)[c]	$\Delta H*$(DMF)[d]
2 (**2**) + **10** → **3**	−30.7	−34.8	−32.9	−36.0
3 → **TS4**	24.8	25.8	25.6	26.6
3 → **5**	10.0	12.4	10.1	12.3
3 + **10** → **TS6**	25.4	22.0	25.5	22.0
3 + **10** → **7**	7.7	8.6	7.1	7.8
7 → **TS8**	22.8	14.5	23.6	15.3
7 → **9** + **11**	−4.7	−0.6	−6.0	−1.9

[a]Energies shown in kcal mol^{-1}. Thermal correction to the enthalpy (H_{corr}) computed with B3LYP in the gas phase. Energy values include ZPVE correction. [b]H = E[M06-L(gas)] + H_{corr}. [c]H = E[B3LYP-(DMF)] + H_{corr}. [d]H = E[M06-L(DMF)] + H_{corr}.

the M06-L functional was designed for use with transition metals,[65,78] we chose to utilize it for comparison to our B3LYP values. Overall we find that enthalpies computed in solvent with the M06-L functional yield a description of the potential energy surface that is more consistent with experiment, but both functionals yield roughly the same trend in enthalpies across the reaction coordinate. Using both functionals, we also find that the change in energy as a result of including an implicit solvent model (CPCM) is small for each reaction step (<1.5 kcal mol^{-1}), which is in part a consequence of all species being charge-neutral. For comparison, we briefly discuss the reaction pathways with regard to results from solvated enthalpies computed with B3LYP and M06-L.

For the formation of carboxylate dimer, the step 2 (**2**) + **10** → **3**, B3LYP yields an enthalpy that is roughly 3 kcal mol^{-1} higher than that obtained with M06-L (−32.9 vs −36.0 kcal mol^{-1}). This trend persists in the activation barrier for insertion, with B3LYP returning a value 3.5 kcal mol^{-1} higher than M06-L (25.5 vs 22.0 kcal mol^{-1}). For the barrier to isomerization, however, both functionals yield a relatively similar value, deviating by only 1 kcal mol^{-1}. As a result, B3LYP predicts a 0.1 kcal mol^{-1} preference for the insertion route rather than isomerization. On the other hand, M06-L gives a larger difference of 4.7 kcal mol^{-1}. There is little experimental evidence for the formation of the axial−equatorial dimer, **5**, and the high barrier to isomerization, especially with respect to the insertion pathway, is aligned with the M06-L results.

Following the insertion pathway, we find that for the activation barrier to rearrangement, the step **7** → **TS8**, B3LYP and M06-L values deviate substantially, at 23.6 vs 15.3 kcal mol^{-1}, respectively. Given that with B3LYP the barrier to isomerization is roughly equal to the activation barrier for both insertion and isomerization steps, those processes would likely be slow, if not prohibited, under the reaction conditions. On the other hand, the decreased barrier for rearrangement using M06-L generally agrees with the experimental observation that rearrangement is not a rate-limiting step, and **7** is not a long-lived intermediate. Both functionals predict rearrangement to be overall exothermic, but B3LYP returns a value roughly 4 kcal mol^{-1} lower than M06-L (−6.0 vs −1.9 kcal mol^{-1}).

SUMMARY

We have investigated the production of CO from a CO_2-saturated solution containing reduced rhenium complexes. Using density functional theory, we have proposed a pathway involving CO_2 insertion into a long-lived carboxylate dimer intermediate. This pathway generally agrees with the experimentally observed products described by Sullivan and co-workers and Hayashi and co-workers. Furthermore, our mechanism aligns with labeling studies performed by the latter. From our investigation, we propose the formation of a stable [Re(dmb)$(CO)_3]_2$(OCO) intermediate via the two-electron reduction of CO_2. The high barrier to isomerization of this dimer and the significant exothermicity of the formation step support the long-lived nature of this species. In the presence of CO_2, [Re(dmb)$(CO)_3]_2$(OCO) undergoes attack via the insertion of CO_2 into the rhenium−oxygen bond. Subsequent rearrangement produces CO and [Re(dmb)$(CO)_3]_2(OCO_2)$, both experimentally observed products. The insertion step also agrees with the kinetic dependence on the concentration of [Re(dmb)$(CO)_3]_2$(OCO) and CO_2 for the production of CO. We find that from the reduced monomer, Re(dmb)$(CO)_3^{\bullet}$, and 2 equiv of CO_2, the overall reaction is exothermic by −30.2 kcal mol^{-1}, with the largest barrier being that of insertion at 21.9 kcal mol^{-1}.

ASSOCIATED CONTENT

Supporting Information

Complete refs 4 and 56, and data for computed stationary points. This material is available free of charge via the Internet at http://pubs.acs.org.

AUTHOR INFORMATION

Corresponding Author

fri@uga.edu; muckerma@bnl.gov

Notes

The authors declare no competing financial interest.

ACKNOWLEDGMENTS

The work at Brookhaven National Laboratory is funded under contract DE-AC02-98CH10886 with the U.S. Department of Energy (DOE) and supported by its Division of Chemical Sciences, Geosciences, & Biosciences, Office of Basic Energy Sciences. E.F. and J.T.M. also thank the DOE for funding under the BES Solar Energy Utilization Initiative. Research at Georgia was supported by the National Science Foundation, Grant CHE-1054286.

REFERENCES

(1) Matthews, H. D.; Gillett, N. P.; Stott, P. A.; Zickfeld, K. *Nature* **2009**, *459*, 829−832.

(2) Melillo, J. M.; McGuire, A. D.; Kicklighter, D. W.; Moore, B.; Vorosmarty, C. J.; Schloss, A. L. *Nature* **1993**, *363*, 234−240.
(3) Schimel, D. S. *Glob. Change Biol.* **1995**, *1*, 77−91.
(4) Gurney, K. R.; et al. *Nature* **2002**, *415*, 626−630.
(5) Stauffer, B.; Blunier, T.; Dallenbach, A.; Indermuhle, A.; Schwander, J.; Stocker, T. F.; Tschumi, J.; Chappellaz, J.; Raynaud, D.; Hammer, C. U.; Clausen, H. B. *Nature* **1998**, *392*, 59−62.
(6) Khatiwala, S.; Primeau, F.; Hall, T. *Nature* **2009**, *462*, 346−349.
(7) Retallack, G. J. *Nature* **2001**, *411*, 287−290.
(8) Meinshausen, M.; Meinshausen, N.; Hare, W.; Raper, S. C. B.; Frieler, K.; Knutti, R.; Frame, D. J.; Allen, M. R. *Nature* **2009**, *458*, 1158−1162.
(9) Schwarz, H. A.; Dodson, R. W. *J. Phys. Chem.* **1989**, *93*, 409−414.
(10) Meshitsuka, S.; Ichikawa, M.; Tamaru, K. *J. Chem. Soc., Chem. Commun.* **1974**, 158−159.
(11) Fisher, B. J.; Eisenberg, R. *J. Am. Chem. Soc.* **1980**, *102*, 7361−7363.
(12) Beley, M.; Collin, J. P.; Ruppert, R.; Sauvage, J. P. *J. Am. Chem. Soc.* **1986**, *108*, 7461−7467.
(13) Simón-Manso, E.; Kubiak, C. P. *Organometallics* **2005**, *24*, 96−102.
(14) Fujita, E.; Haff, J.; Sanzenbacher, R.; Horst, E. *Inorg. Chem.* **1994**, *33*, 4627−4628.
(15) Kelly, C. A.; Mulazzani, Q. G.; Venturi, M.; Blinn, E. L.; Rodgers, M. A. J. *J. Am. Chem. Soc.* **1995**, *117*, 4911−4919.
(16) Kelly, C. A.; Blinn, E. L.; Camaioni, N.; D'Angelantonio, M.; Mulazzani, Q. G. *Inorg. Chem.* **1999**, *38*, 1579−1584.
(17) Fujita, E.; Brunschwig, B. S.; Ogata, T.; Yanagida, S. *Coord. Chem. Rev.* **1994**, *132*, 195−200.
(18) Behar, D.; Dhanasekaran, T.; Neta, P.; Hosten, C. M.; Ejeh, D.; Hambright, P.; Fujita, E. *J. Phys. Chem. A* **1998**, *102*, 2870−2877.
(19) Morris, A. J.; Meyer, G. J.; Fujita, E. *Acc. Chem. Res.* **2009**, *42*, 1983−1994.
(20) Fujita, E.; Creutz, C.; Sutin, N.; Szalda, D. J. *J. Am. Chem. Soc.* **1991**, *113*, 343−353.
(21) Creutz, C.; Schwarz, H. A.; Wishart, J. F.; Fujita, E.; Sutin, N. *J. Am. Chem. Soc.* **1991**, *113*, 3361−3371.
(22) Fujita, E.; Creutz, C.; Sutin, N.; Brunschwig, B. S. *Inorg. Chem.* **1993**, *32*, 2657−2662.
(23) Matsuoka, S.; Yamamoto, K.; Ogata, T.; Kusaba, M.; Nakashima, N.; Fujita, E.; Yanagida, S. *J. Am. Chem. Soc.* **1993**, *115*, 601−609.
(24) Ogata, T.; Yanagida, S.; Brunschwig, B. S.; Fujita, E. *J. Am. Chem. Soc.* **1995**, *117*, 6708−6716.
(25) Khenkin, A.; Efremenko, I.; Weiner, L.; Martin, J.; Neumann, R. *Chem.—Eur. J.* **2010**, *16*, 1356−1364.
(26) Tanaka, K.; Ooyama, D. *Coord. Chem. Rev.* **2002**, *226*, 211−218.
(27) Kitamura, N.; Tazuke, S. *Chem. Lett.* **1983**, *7*, 1109−1112.
(28) Ishida, H.; Tanaka, K.; Tanaka, T. *Chem. Lett.* **1988**, *6*, 339−342.
(29) Ishida, H.; Terada, T.; Tanaka, K.; Tanaka, T. *Inorg. Chem.* **1990**, *29*, 905−911.
(30) Tinnemans, A. H. A.; Koster, T. P. M; Thewissen, D. H. M.W.; Mackor, A. *Recl. Trav. Chim. Pays-Basque* **1984**, *103*, 288−295.
(31) Kimura, E.; Wada, S.; Shionoya, M.; Okazaki, Y. *Inorg. Chem.* **1994**, *33*, 770−778.
(32) Maidan, R.; Willner, I. *J. Am. Chem. Soc.* **1986**, *108*, 8100−8101.
(33) Hayashi, Y.; Kita, S.; Brunschwig, B.; Fujita, E. *J. Am. Chem. Soc.* **2003**, *125*, 11976−11987.
(34) Gibson, D. H. *Coord. Chem. Rev.* **1999**, *185*−*6*, 335−355.
(35) Johnson, F. P. A; George, M. W.; Hartl, F.; Turner, J. J. *Organometallics* **1996**, *15*, 3374−3387.
(36) Doherty, M. D.; Grills, D. C.; Fujita, E. *Inorg. Chem.* **2009**, *48*, 1796−1798.
(37) Doherty, M. D.; Grills, D. C.; Muckerman, J. T.; Polyansky, D. E.; Fujita, E. *Coord. Chem. Rev.* **2010**, *254*, 2472−2482.
(38) Schneider, J.; Vuong, K. Q.; Calladine, J. A.; Sun, X.-Z.; Whitwood, A. C.; George, M. W.; Perutz, R. N. *Inorg. Chem.* **2011**, *50*, 11877−11889.
(39) Grodkowski, J.; Neta, P. *J. Phys. Chem. A* **2000**, *104*, 4475−4479.
(40) Grodkowski, J.; Behar, D.; Neta, P.; Hambright, P. *J. Phys. Chem. A* **1997**, *101*, 248−254.
(41) Dhanasekaran, T.; Grodkowski, J.; Neta, P.; Hambright, P.; Fujita, E. *J. Phys. Chem. A* **1999**, *103*, 7742−7748.
(42) Takeda, H.; Koike, K.; Inoue, H.; Ishitani, O. *J. Am. Chem. Soc.* **2008**, *130*, 2023−2031.
(43) Takeda, H.; Ishitani, O. *Coord. Chem. Rev.* **2010**, *254*, 346−354.
(44) Gholamkhass, B.; Mametsuka, H.; Koike, K.; Tanabe, T.; Furue, M.; Ishitani, O. *Inorg. Chem.* **2005**, *44*, 2326−2336.
(45) Bian, Z.-Y.; Sumi, K.; Furue, M.; Sato, S.; Koike, K.; Ishitani, O. *Dalton Trans.* **2009**, 983−993.
(46) Whitten, D. G. *Acc. Chem. Res.* **1980**, *13*, 83−90.
(47) Ogata, T.; Yamamoto, Y.; Wada, Y.; Murakoshi, K.; Kusaba, M.; Nakashima, N.; Ishida, A.; Takamuku, S.; Yanagida, S. *J. Phys. Chem.* **1995**, *99*, 11916−11922.
(48) Richardson, R. D.; Carpenter, B. K. *J. Am. Chem. Soc.* **2008**, *130*, 3169−3180.
(49) Carpenter, B. K. *J. Phys. Chem. A* **2007**, *111*, 3719−3726.
(50) Agarwal, J.; Johnson, R. P.; Li, G. *J. Phys. Chem. A* **2011**, *115*, 2877−2881.
(51) Sullivan, B. P.; Bolinger, C. M.; Conrad, D.; Vining, W. J.; Meyer, T. J. *J. Chem. Soc., Chem. Commun.* **1985**, 1414−1416.
(52) Fujita, E.; Muckerman, J. T. *Inorg. Chem.* **2004**, *43*, 7636−7647.
(53) Gibson, D. H.; Yin, X. L.; He, H. Y.; Mashuta, M. S. *Organometallics* **2003**, *22*, 337−346.
(54) Smieja, J. M.; Kubiak, C. P. *Inorg. Chem.* **2010**, *49*, 9283−9289.
(55) Kumar, B.; Smieja, J. M.; Kubiak, C. P. *J. Phys. Chem. C* **2010**, *114*, 14220−14223.
(56) Frisch, M. J. et al. *Gaussian 09*, Revision B.01; Gaussian Inc.: Wallingford, CT, 2009.
(57) Barone, V.; Cossi, M. *J. Phys. Chem. A* **1998**, *102*, 1995−2001.
(58) Cossi, M.; Rega, N.; Scalmani, G.; Barone, V. *J. Comput. Chem.* **2003**, *24*, 669−681.
(59) Fukui, K. *Acc. Chem. Res.* **1981**, *14*, 363−368.
(60) Hratchian, H. P.; Schlegel, H. B. *J. Chem. Phys.* **2004**, *120*, 9918−9924.
(61) Hratchian, H. P.; Schlegel, H. B. *J. Chem. Theory Comput.* **2005**, *1*, 61−69.
(62) Becke, A. D. *J. Chem. Phys.* **1993**, *98*, 5648−5652.
(63) Becke, A. D. *J. Chem. Phys.* **1996**, *104*, 1040−1046.
(64) Lee, C. T.; Yang, W. T.; Parr, R. G. *Phys. Rev. B* **1988**, *37*, 785−789.
(65) Zhao, Y.; Truhlar, D. G. *J. Chem. Phys.* **2006**, *125*, 194101.
(66) Sieger, M.; Kaim, W.; Stufkens, D. J.; Snoeck, T. L.; Stoll, H.; Záliš, S. *Dalton Trans.* **2004**, *22*, 3815−3821.
(67) Roy, L. E.; Hay, P. J.; Martin, R. L. *J. Chem. Theory Comput.* **2008**, *4*, 1029−1031.
(68) Pantazis, D. A.; Neese, F. *J. Chem. Theory Comput.* **2009**, *5*, 2229−2238.
(69) Choua, S.; Djukic, J.; Dalléry, J.; Bieber, A.; Welter, R. *Inorg. Chem.* **2008**, *48*, 149−163.
(70) Cramer, C. J.; Truhlar, D. G. *Phys. Chem. Chem. Phys.* **2009**, *11*, 10757−10816.
(71) Li, X.; Liu, X.; Wu, Z.; Zhang, H. *J. Phys. Chem. A* **2008**, *112*, 11190−11197.
(72) Rodríguez, L.; Ferrer, M.; Rossell, O.; Duarte, F. J. S.; Santos, A. G.; Lima, J. C. *J. Photochem. Photobiol. A* **2009**, *204*, 174−182.
(73) Radosevich, A. T.; Melnick, J. G.; Stoian, S. A.; Bacciu, D.; Chen, C.-H.; Foxman, B. M.; Ozerov, O. V.; Nocera, D. G. *Inorg. Chem.* **2009**, *48*, 9214−9221.
(74) Dill, J. D.; Pople, J. A. *J. Chem. Phys.* **1975**, *62*, 2921−2923.
(75) Francl, M. M.; Pietro, W. J.; Hehre, W. J.; Binkley, J. S.; Gordon, M. S.; Defrees, D. J.; Pople, J. A. *J. Chem. Phys.* **1982**, *77*, 3654−3665.
(76) Sullivan, B. P.; Meyer, T. J. *Organometallics* **1986**, *5*, 1500−1502.
(77) Tryk, D. A.; Yamamoto, T.; Kokubun, M.; Hirota, K.; Hashimoto, K.; Okawa, M.; Fujishima, A. *Appl. Organomet. Chem.* **2001**, *15*, 113−120.

(78) Zhao, Y.; Truhlar, D. G. *Theor. Chem. Acc.* **2008**, *120*, 215−241.

dx.doi.org/10.1021/ja2105834 | *J. Am. Chem. Soc.* 2012, 134, 5180−5186